# PICOSECOND AND SUB-PICOSECOND, HIGH CHARGE ELECTRON LINACS[*]

A. M. M. Todd, H. P. Bluem, C. C. Paulson, M. F. Reusch and I. S. Lehrman[a]

Northrop Grumman Advanced Systems & Technology,
9 Jeffrey Lane, Princeton Junction, New Jersey 08550, USA

## Abstract

We have built and are presently designing, photocathode-based accelerator systems for radiation chemistry applications. One of these accelerators is in operation at Brookhaven National Laboratory. All feature a photocathode electron gun and produce a short, intense electron pulse with a variable repetition rate. The designs range from 1 nC to 100 nC per pulse, with bunch lengths of 0.6 psec at lower charge levels to less than 50 psec at higher charge. A compact design which can deliver 10 nC of charge in less than 5 psec and a larger machine designed to deliver up to 100 nC of charge in less than 50 psec, are described. Data on the operating system is also presented.

## 1 INTRODUCTION

Linear accelerators based upon photocathode RF electron guns are ideally suited for a number of scientific applications. The unique properties of these systems include the ability to produce a single, intense pulse of electrons at a variable repetition rate whose timing can be precisely controlled. These electrons can be used directly, through a thin window, or to generate an intense burst of gamma rays.

For the past few years, we have been designing photocathode-based linacs for scientific research [1]. In particular, we have delivered one accelerator beamline to Brookhaven National Laboratory (BNL) for pulse radiolysis chemistry research, and have designed two others for similar applications. The installed accelerator has been operating successfully for almost two years, producing in excess of 10 nC per pulse. The design and performance of this accelerator follows. Thereafter, the other two designs with their differing performance and packaging, are described.

## 2 BNL SYSTEM PERFORMANCE

The machine presently in operation at Brookhaven includes two beamlines. The first is a beamline deflected 90 degrees from the straight path, and the other is a beamline along the straight path. Two further deflected path beamlines can be installed. The electrons are delivered to one beamline or the other through energization of the bend magnets.

The bent path fulfills several important functions. Firstly, when properly designed, it provides a certain amount of longitudinal bunch compression which leads to higher peak current and better time resolution. The bent path can also be used for energy analysis of the electrons, if desired, and provides excellent suppression of the dark current due to energy selectivity.

The electron source is a 3.5 cell S-band photocathode RF gun which can produce electron energies up to 9 MeV. The electrons are produced in a single microbunch through illumination of the photocathode with a picosecond laser pulse synchronized to the RF that drives the gun cavities. A variable laser pulse width can be used to tailor the electron bunches to suit the needs of the experiment. The system runs at a repetition rate of 10 Hz, but this is not a fundamental limit. Quadrupole, dipole steering, and dipole bending magnets transport the electron pulse to the desired target.

The system has achieved the design goals that correspond to the present photocathode drive laser performance. The deflected beamline was designed to produce 10 nC bunches with a pulse width of less than 5 psec on target. The straight beamline was specified to deliver greater than 20 nC with pulse lengths of less than 30 psec. The transverse spot size on both targets can be varied over a wide range. To date, up to 12 nC have been delivered to both target stations with laser energies of 180 μJ per pulse. The dark current on the deflected path is measured to be less than 0.1 nC summed over the entire 4 μsec RF pulse.

## 3 NEW DESIGNS

Two new but related designs, with very different performance parameters, have recently been developed. The first is a very compact machine with only two target stations. The second machine is much larger and presently envisages five target stations.

The compact design is very similar to the BNL machine. An S-band 3.5 cell gun produces the 9 MeV electron pulses. These pulses can be delivered to one of two target stations via either a straight path or a bent

---

[a] Present address: General Instrument Corporation, 101 Tournament Drive, Horsham, PA 19044, USA.

path. The pulses contain over 10 nC in a FWHM length of less than 10 psec on the straight path, and less than 5 psec on the bent path. The entire beamline, from the gun to the target stations, fits onto an optical table with dimensions of 2 meters by 3 meters.

The final design is a significant departure from the two previously described systems. It was driven by two separate goals, namely, very high charge and very short bunch lengths.

Achieving much higher charge necessitated a switch to an L-band accelerator. Operation of the gun in L-band allows a longer laser pulse and a larger laser spot size before beam quality starts degrading significantly. The longer pulse and larger spot allow more charge to be extracted before charge shielding becomes a major issue. They also allow more laser energy to be incident upon the cathode without exceeding the maximum permissible intensity.

To make it possible to attain the shorter bunches, the design includes a four cell booster accelerator after the 2.5 cell photocathode electron gun. The booster's RF phase is used to adjust the electrons longitudinal phase space in order to achieve optimal compression in the subsequent magnetic pulse compressor. In addition, the gun has been designed to provide a nearly linear relationship in longitudinal phase space. Through careful matching of the gun and booster, compression ratios of around 15 between the output of the gun and the end of the beamline have been achieved.
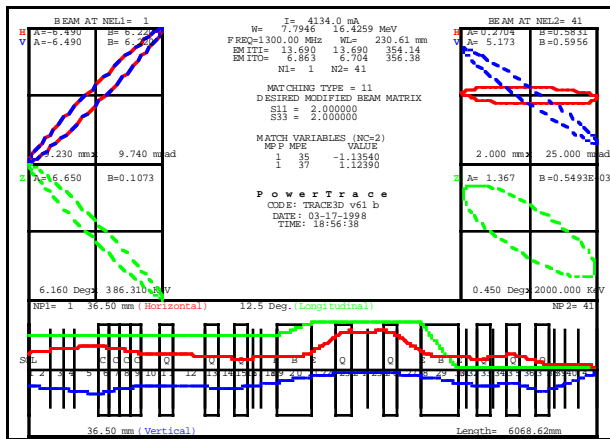


Figure 1. L-Band system beamline envelopes at 3.2 nC.

Figure 1 is a TRACE-3D [2] illustration of the beamline envelopes, showing the bunch compression. Nonlinear analysis of the beam on target using the TOPKARK [3] code yields, after aperturing, the transverse and longitudinal phase space plots of Figure 2.

The booster accelerator also assists in achieving the high charge operation. This is because, given a fixed amount of available RF power, the shorter gun can be operated at a higher gradient than would be possible with a longer gun. The gun and booster produce electron pulses up to an energy of 15 MeV while allowing the gun to be

operated at maximum gradients. A higher gradient in the gun both raises the threshold for charge shielding considerations and raises the effective quantum efficiency of the cathode through the Schottky effect.
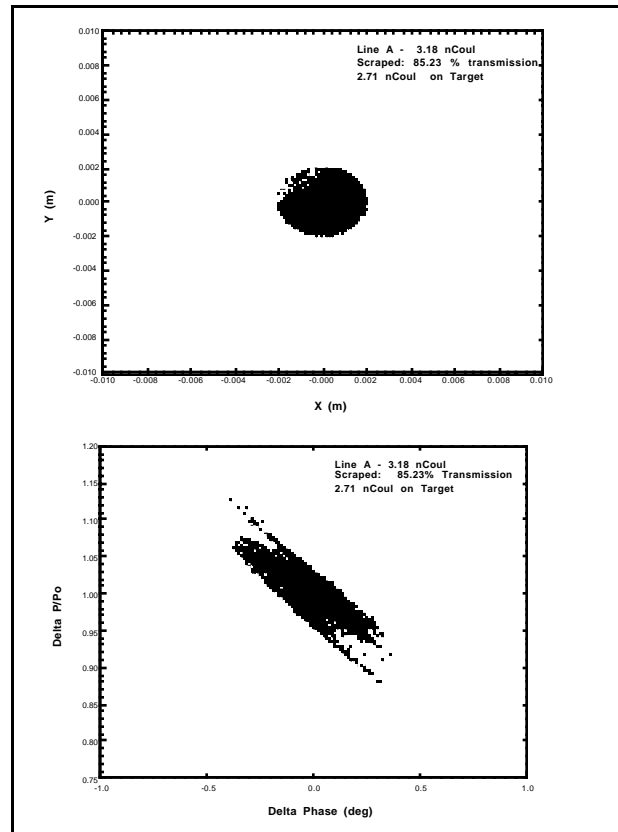


Figure 2. Transverse (upper) and longitudinal (lower) phase space plots for a 2 mm apertured, 2.7 nC, 0.67 psec FWHM bunch.

The beamline has multiple target stations, as shown in Figure 3, and the layout was designed to fit into an existing facility.
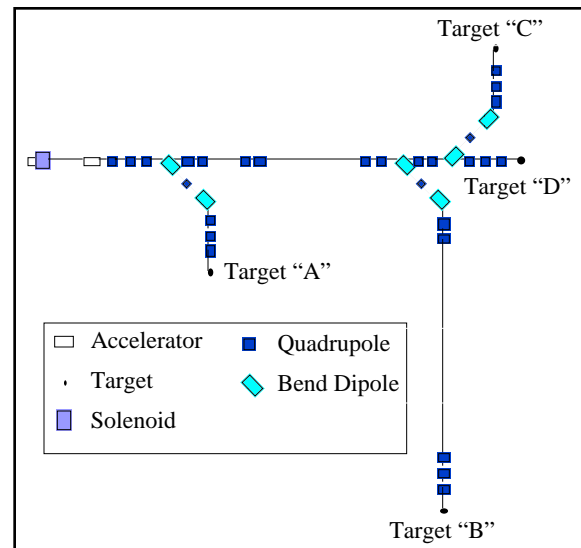


Figure 3. Four target L-band beamline layout.

The closest target to the accelerator, "A", is optimized for short pulse operation. Also, it is intended that the electron pulse at this target be synchronized with a sample of the photocathode drive laser to provide precise timing for pump-probe type experiments. At this target station, a pulse length of 0.67 psec FWHM has been achieved with 2.7 nC on target after aperturing a 3.2 nC beam and focusing the electrons to a transverse spot size of 2 mm radius. Lesser charge can be delivered in even shorter pulse lengths, while a 10 nC bunch can be compressed to less than 2 psec FWHM. At this target, we have achieved, in our non-linear simulations, peak currents in excess of 5 kA and peak densities in excess of 30 kA/cm$^2$.

The other two target stations on bent paths cannot match the performance of target "A" due to their distance away from the accelerator, smaller space for the achromat, and the necessity to have long sections of drift space. They were designed primarily to transport the high charge pulses.

The gun can produce up to 100 nC depending upon the available laser energy. After acceleration in the booster, this current can be delivered to either the first target station or any of the other targets. At target "A", the transport efficiency for the high charges approaches 100% and the pulse length can be compressed to less than 20 psec FWHM for 90 nC. The other two targets on bent paths have transport efficiencies of 81% and 89% with pulse lengths of around 25 psec FWHM. For comparison, the straight path target "D" has close to 100% transport with a pulse length of a little over 50 psec. A summary of the on-target performance at each of the four target stations is shown in Table 1.

## 4 SUMMARY

Northrop Grumman has built or designed three state-of-the-art electron accelerators. Although all three designs were driven by chemistry research applications, accelerators of this type have a much broader range of applications. These accelerators, based upon photocathode RF guns, can deliver very intense, very short (sub-picosecond) pulses of electrons or longer (20-30 psec), very high single bunch charge. The accelerator presently in use has met or exceeded all expectations.

## ACKNOWLEDGMENTS

## REFERENCES

[1] e.g. I. S Lehrman, et al., "Design and Operation of the Compact Infrared Free Electron Laser (CIRFEL)," Electron-Beam Sources and Charged-Particle Optics, Proceedings of the SPIE, Eric Munro and Henry Freund, Eds., 2522 (1995) 451.

[2] K. R. Crandall and D. P. Rusthoi, "TRACE-3D Documentation, Third Edition," Los Alamos National Laboratory Report LA-UR-97-886 (May 1997).

[3] D. L. Bruhwiler and M. F. Reusch, "High-Order Optics with Space Charge: The TOPKARK Code," Computational Accelerator Physics, AIP Conf. Proc. **297** (1993) 524.

| ID # | Target | Energy (MeV) | Charge (nC) | X FWHM (mm) | Y FWHM (mm) | T FWHM (psec) |
|---|---|---|---|---|---|---|
| 5 | A | 16.11 | 3.2 | 2.6 | 2.6 | 0.87 |
| *6* | *A* | *16.11* | *2.7* | *2.0* | *2.0* | *0.67* |
| 7 | A | 16.08 | 10.2 | 3.8 | 2.0 | 1.90 |
| *8* | *A* | *16.83* | *87.2* | *4.7* | *5.4* | *19.6* |
| 9 | B | 16.54 | 3.0 | 5.7 | 0.7 | 3.61 |
| 10 | B | 17.87 | 10.0 | 13.3 | 4.2 | 5.04 |
| 11 | B | 16.42 | 72.9 | 7.4 | 3.5 | 27.73 |
| 13 | C | 16.07 | 3.2 | 3.6 | 5.9 | 1.92 |
| 14 | C | 17.26 | 10.2 | 4.1 | 1.7 | 3.72 |
| *15* | *C* | *16.48* | *80.1* | *5.3* | *5.3* | *25.81* |
| 16 | D | 16.03 | 3.2 | 1.2 | 1.5 | 16.29 |
| 17 | D | 16.49 | 10.2 | 2.7 | 5.0 | 13.31 |
| 18 | D | 16.45 | 89.1 | 4.8 | 3.8 | 51.53 |

Table 1. Summary of on-target performance simulations